Labeling the Defects of Single-Walled Carbon Nanotubes Using Titanium Dioxide Nanoparticles

Xiaohong Li, Jiali Niu, Jin Zhang,* Hulin Li,† and Zhongfan Liu*

Center for Nanoscale Science and Technology (CNST), College of Chemistry & Molecular Engineering, Peking University, Beijing 100871, P. R. China

Received: August 30, 2002

We describe here a new method for labeling the defects of single-walled carbon nanotubes (SWNTs) using TiO_2 nanoparticles as markers. SWNTs were prepared by chemical vapor deposition, and dilute nitric acid (2.6M) oxidation was used to introduce carboxylic acid groups at the defect sites. Characterization of the SWNTs using ultrastructural and spectroscopic analyses was carried out following introduction of TiO_2 nanoparticles. The results indicated that TiO_2 nanoparticles were chemically absorbed at SWNT defect sites via an ester-type linkage between carboxylic acid groups at the defect sites and hydroxyl groups at the surface of the TiO_2 nanoparticles. In addition, the adsorption behavior of TiO_2 nanoparticles on SWNTs was determined following oxidization of the SWNTs using different processes. The results indicated that gas-phase oxidation introduces very few defect sites as evidenced by the low adsorption density of TiO_2 nanoparticles. Refluxing in dilute nitric acid can be considered as a mild oxidation for SWNTs, affecting only those defects already present and causing no further damage. In contrast, sonication of SWNTs in H_2SO_4/H_2O_2 increased the incidence of carboxylic acid groups, not only at original defect sites but also at newly created defect sites along the walls of SWNTs, resulting in a higher density of TiO_2 nanoparticles. In conclusion, labeling of SWNT defect sites using TiO_2 nanoparticles permits direct determination of the density, distribution, and location of the defects and offers new possibilities for the creation of heterojunctions between nanotubes and nanoparticles in the future.

Introduction

The potential uses of single-walled carbon nanotubes (SWNTs), for example, in field emission displays,[1,2] nanoelectronic devices (single-electron transistors[3] and field-effect transistors[4]), polymer reinforcement,[5] and attached to atomic force microscopy (AFM) tips for high-resolution studies of biological surfaces[6] has been recognized since their discovery in 1993.[7] However, the preparation, characterization, and functionalization of SWNTs remain complex and difficult. Previous studies have indicated that any disruptions to the local order of SWNTs would strongly influence their properties and behaviors. Theoretical calculations have shown that local structural defects, such as topological defects, vacancies, impurities, and deformations, substantially modify the electronic and transport properties of SWNTs.[8−11] Defects inevitably arise during the growth of SWNTs[12,13] and may also be introduced after some postsynthesis treatments such as chemical etching,[14] ultrasonication,[15] or electron beam irradiation.[16] To further the usefulness of SWNTs, it is therefore essential to understand the distribution, density, and nature of defects on SWNTs, as well as the influence of such defects on their electronic properties.

However, investigations to determine the density, distribution, and location of defects on SWNTs are still in their infancy due to lack of direct and reliable methods to label defect sites. Previous attempts have been made to locate defects on nanotubes using high-resolution TEM,[17] STM,[18] chemical titration,[19] and mid-IR spectroscopy.[20] Using chemical titration, Smally et al.[19] suggested that ∼5% of the carbon atoms in SWNTs were located at defect sites. Similar results were reported by Haddon et al.,[20] using solution phase mid-IR spectroscopy. However, methods such as these provide only an average measure of the defect density in bulk samples. A more recent work by Fan et al.[21] used a simple technique based on the formation of Se nanoparticles on the tubes upon exposure to hydrogen selenide (H_2Se) under ambient conditions to locate the defects on SWNTs which offered the advantage of a more specific characterization of defect density.

Functionalization of carbon nanotubes by chemical oxidation using H_2SO_4/HNO_3, H_2SO_4/H_2O_2, HNO_3, O_3, $KMnO_4$, OsO_4, and RuO_4 has opened up new opportunities for carbon nanotube chemistry[19,22−27] and has added advantage of being able to both modify and study nanotube properties in solution. Chemical oxidation generally results in the production of carboxylic groups at the defect sites located at the ends and/or the side walls of the nanotubes because of the different chemical reactivity between perfect structure and defects. In the present study, we have developed a new method for labeling defects on SWNTs using TiO_2 nanoparticles as markers. TiO_2 nanoparticles were chosen based upon the reported chemical adsorption of carboxylic acid groups onto titanium dioxide surfaces via the formation of ester-like linkages[28,29] as used in solar photoconversion systems.[30−33] In addition, TiO_2 nanoparticles can be readily located using AFM or SEM, and the labeling process itself is relatively rapid and simple compared with other methods.[19,20] This new approach therefore permits the direct observation of the density, distribution, and location of SWNT defects. Using this method, we have been able to investigate the location of TiO_2 nanoparticles on SWNTs functionalized using different oxidation processes to further our understanding of the mechanism of oxidation of SWNTs.

* To whom correspondence should be addressed. Fax: 00-86-10-6275-7157. E-mail: jzhang@chem.pku.edu.cn; lzf@chem.pku.edu.cn.

† Chemistry Department of Lanzhou University, Lanzhou 730000, P. R. China.

10.1021/jp026887y CCC: $25.00
Published on Web 02/21/2003

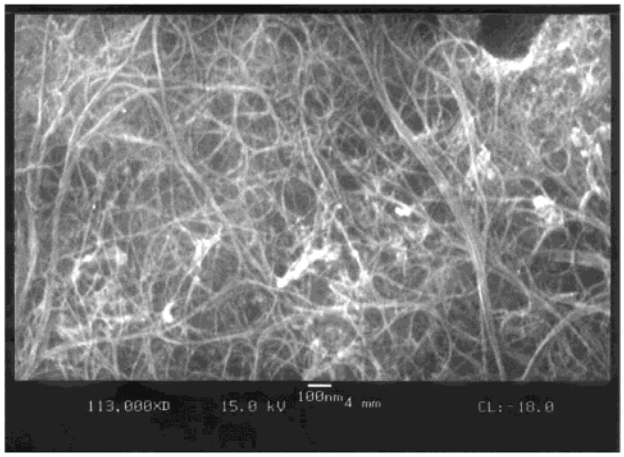

Figure 1. Typical SEM image of the purified SWNTs.

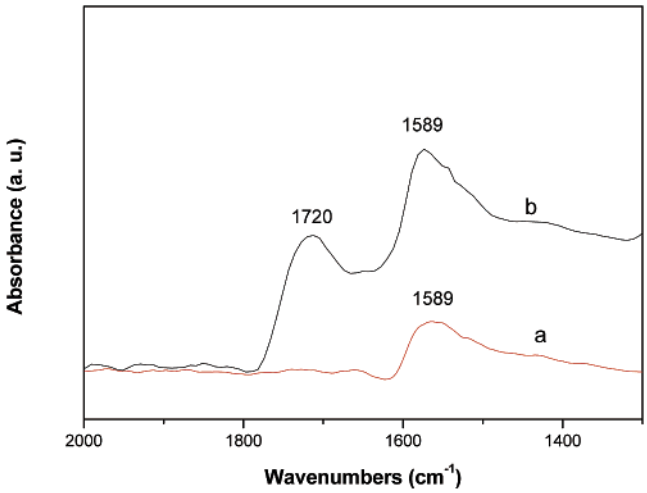

Figure 2. FTIR spectra of the SWNTs before (a) and after refluxing in 2.6 M HNO_3 (b).

Experimental Section

TiO_2 nanoparticles were synthesized by adding 25 mL of tetrabutyl titanate dropwise to 300 mL of HNO_3 solution (pH = 1) while vigorously stirring. The solution was then incubated at 80 °C for 8 h with continued stirring. After leaving it to settle at room temperature for 7 days, a stable colloidal dispersion of TiO_2 was obtained.[34]

SWNTs were produced using the CVD method, described in detail elsewhere.[35] Using CVD methodology, the resulting impurities in the as-prepared SWNTs product were mainly amorphous carbon and catalyst particles. The catalyst (support and metal particles) can be removed by sonicating in 37 wt % hydrochloric acid for 30 min, leaving in the acid overnight, and then diluting with deionized water followed by filtration through ϕ0.1 μm Supor membrane disk filters (Gelman). Figure 1 shows a typical SEM image of the purified SWNTs prepared using this method. Abundant rope-like nanotube networks can be observed, with little evidence of contaminants, indicating that the product consists of relatively high-purity SWNTs.

The SWNTs preparations were then treated with one of three different oxidation processes: refluxing SWNTs in 2.6 M HNO_3 for 30 h, gas-phase oxidation in air at 500 °C for 1 h, and sonicating SWNTs in H_2SO_4/H_2O_2 (4:1 by volume) for 0.5 h. Each of these methods leads to the formation of oxygen-containing groups at defect sites of SWNTs to a greater or lesser extent. The oxidized SWNTs were then dispersed in dimethylformamine (DMF), forming a pale, brown-colored

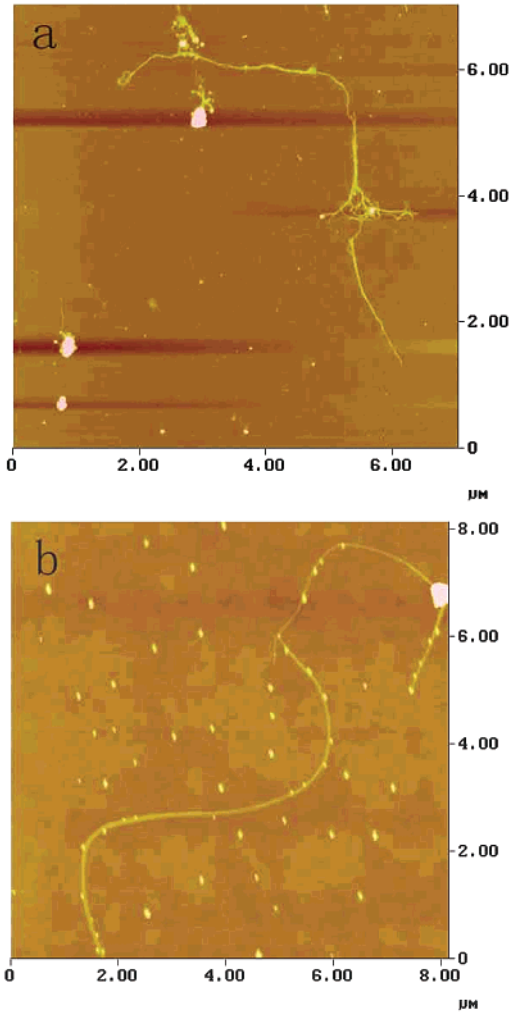

Figure 3. Typical tapping mode AFM images of the location of TiO_2 nanoparticles on SWNTs before (a) and after refluxing in 2.6 M HNO_3 (b).

SCHEME 1: Schematic Illustration of the Basic Methodology for Labeling the Defects on SWNTs Using TiO_2 Nanoparticles as Markers

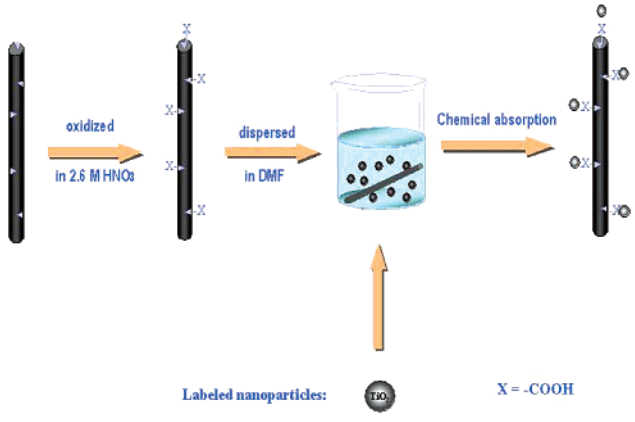

suspension. Scheme 1 shows an overview of the basic methodology for locating defects on SWNTs using TiO_2 nanoparticles as markers. The defect sites on SWNTs are preferentially oxidized to terminal carboxylic acid groups because they are more reactive than perfect sites.[36] A certain amount of TiO_2 nanoparticles was then added into the suspension of SWNTs, and the mixture was ultrasonicated for 30 min before being deposited on a Si wafer.

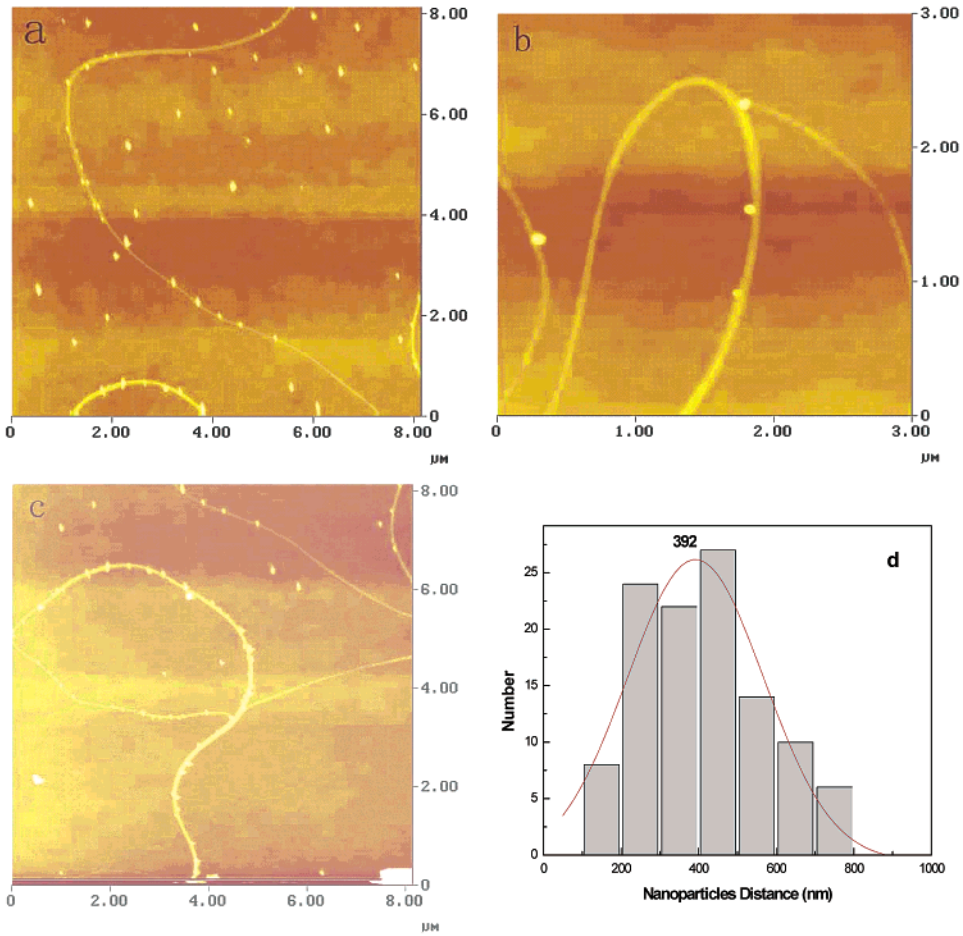

Figure 4. AFM images of the location of TiO_2 nanoparticles on SWNTs after refluxing in 2.6 M HNO_3 (a), of a magnified view (b), of the location of TiO_2 nanoparticles on the thicker bundles of SWNTs (c), and the corresponding histogram of the TiO_2 nanoparticle distances (d). The solid lines correspond to Gaussian fits.

The morphology and microstructure of the SWNTs were characterized using AFM and SEM. AFM characterization was performed on a NanoscopeIII (Digital Instrument, USA) in tapping mode. SEM was conducted at 25 kV using a Hitachi H-800 field-emission instrument. Raman characterization was conducted on a Renishaw System 1000 Raman imaging system equipped with a 632.8 nm, 25 mW He−Ne laser. The IR spectra were obtained by using a Nicolet AVATAR-360 Fourier transform infrared (FTIR) spectrometer.

Results and Discussion

Figure 2 shows the IR spectra of the SWNTs before (a) and after (b) refluxing in 2.6 M HNO_3. Both of the spectra show a peak at 1589 cm^{-1}, corresponding to the IR active phonon mode of SWNTs.[20] After refluxing in 2.6 M HNO_3, a new peak around 1720 cm^{-1} was apparent, corresponding to the stretch mode of carboxylic acid groups[24]. This indicated that carboxylic acid groups had formed at both of the ends and sidewalls of the SWNTs after refluxing in HNO_3.

Figure 3 shows typical tapping mode AFM images of the SWNTs following attachment of TiO_2 nanoparticles before (a) and after (b) refluxing in 2.6 M HNO_3. No TiO_2 nanoparticles were detected on SWNTs before refluxing (Figure 3a). In contrast, TiO_2 nanoparticles appeared to have attached selectively to SWNT surfaces after refluxing, with nonequal spacing along the tubes or thin bundles. Based upon measurements from the AFM section profiles, the oxidized SWNTs present as individual tubes and thin tube bundles (2−4 nm in height). The TiO_2 nanoparticles are ∼15 nm in height with well-defined dispersion (Figure 3b). TiO_2 nanoparticles tended to be preferentially attached to the ends, the curves, and the connecting regions of the SWNTs, where there is the larger concentration of carboxylic acid groups and, thus, the higher possibility of ester-like formation (Figures 3b and 4a). A closer inspection of higher magnification AFM images revealed that the TiO_2 nanoparticles were in intimate contact with the SWNT surface, positioned sometimes on the nanotube sides and sometimes on top of the tubes (Figure 4b). In addition (see Figure 4c), the density of TiO_2 nanoparticles on the thicker bundles of SWNTs was greater than that on the thinner or individual tubes. This is commensurate with the expectation that the number of defects/carboxylic acid groups on the thicker bundles is greater than that on the thinner bundles because of the aggregate effect.[37]

Figure 4d shows the internanoparticle distances from a large number of AFM images. This distance is interpreted as reflecting the chemical defect density on oxidized SWNTs and should therefore represent the maximum distance over which ballistic electrical transport is possible.[21] The result demonstrates that center-to-center separations of TiO_2 nanoparticles absorbed chemically on oxidized SWNTs fall in the range between 100 and 800 nm, with an average distance of ∼392 nm. This is in close agreement with previous experimentally derived values based on phase coherence length of 150−750 nm.[38,39]

To characterize the interaction between oxidized SWNTs and TiO_2 nanoparticles, FTIR spectroscopy was used. Figure 5 shows FTIR spectra of TiO_2 nanoparticles (a), oxidized SWNTs

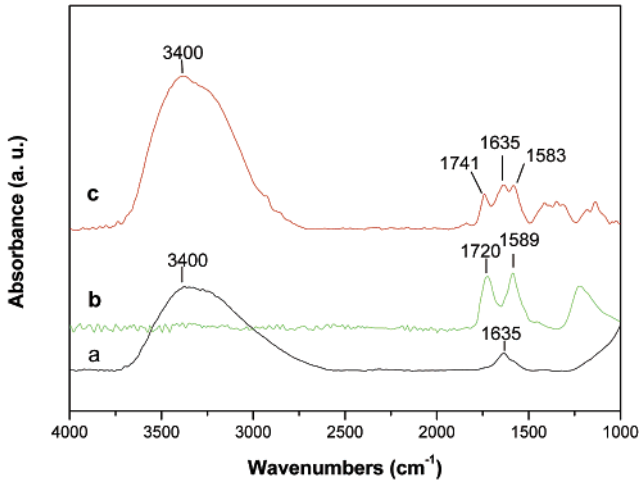

Figure 5. FTIR spectra of TiO_2 nanoparticles (a), oxidized SWNTs (refluxing in HNO_3) before (b) and after absorbed with TiO_2 nanoparticles (c).

(following refluxing in HNO_3) (b), and after adsorption of the oxidized SWNTs with TiO_2 nanoparticles (c). The spectrum of pure TiO_2 nanoparticles showed strong absorbance due to hydroxyl groups around 3400 cm^{-1}. A peak at 1635 cm^{-1} was also observed, which is probably due to the adsorption of undecomposed tetrabutyl titanate. Comparing the spectrum for oxidized SWNTs with that obtained for the oxidized SWNTs following adsorption with TiO_2 nanoparticles revealed that the C═O stretching mode of the carboxylic acid groups had shifted from 1720 to 1741 cm^{-1}. This shift to higher frequency can be explained by the adsorption and binding of oxidized SWNTs onto the TiO_2 nanoparticle surfaces. Furthermore, it is important to note that the peaks at 3400 and 1635 cm^{-1} are present in both of the spectra of pure TiO_2 nanoparticles and TiO_2 nanoparticles absorbed to oxidized SWNTs. The result presents strong evidence for chemical adsorption between surface hydroxyl groups of TiO_2 nanoparticles and carboxylic acid groups contained on oxidized SWNTs via the formation of ester-like binding as predicted.

To further demonstrate the capabilities of this method, we investigated the adsorption of TiO_2 nanoparticles on SWNTs following treatment with different oxidizing processes (see experimental section). Figure 6a shows the SEM image of TiO_2 nanoparticles located on gas phase oxidized SWNTs. Nanoparticles were rarely absorbed on to oxidized SWNTs prepared by this method. The original SWNTs can be seen to have been reduced in length and are relatively "clean" implying that the defect sites on SWNTs (as well as any amorphous carbon impurities) have been eliminated by the gas oxidation process, presumably because defect sites would be more chemically reactive compared with nondefect sites.[21] Further support is provided from Raman spectra. Figure 6b shows the Raman spectra of SWNTs before and after gas-phase oxidation in air at 500 °C for 1 h. Typical SWNT features are observed for the tangential and radial modes near 1590 and 189 cm^{-1}, respectively.[40] The intensity of the peak at 1350 cm^{-1}, which is assigned to the amorphous carbon or fine graphitic particles, was greatly reduced after gas-phase oxidation, indicating that the product consists of high-purity SWNTs. In this regard, the gas oxidation process may be targeted as an effective strategy for the efficient cutting and purification of SWNTs.

Figure 7a shows the SEM image of TiO_2 nanoparticles located on SWNTs previously oxidized by sonication in H_2SO_4/H_2O_2. The density of absorbed nanoparticles is obviously higher than

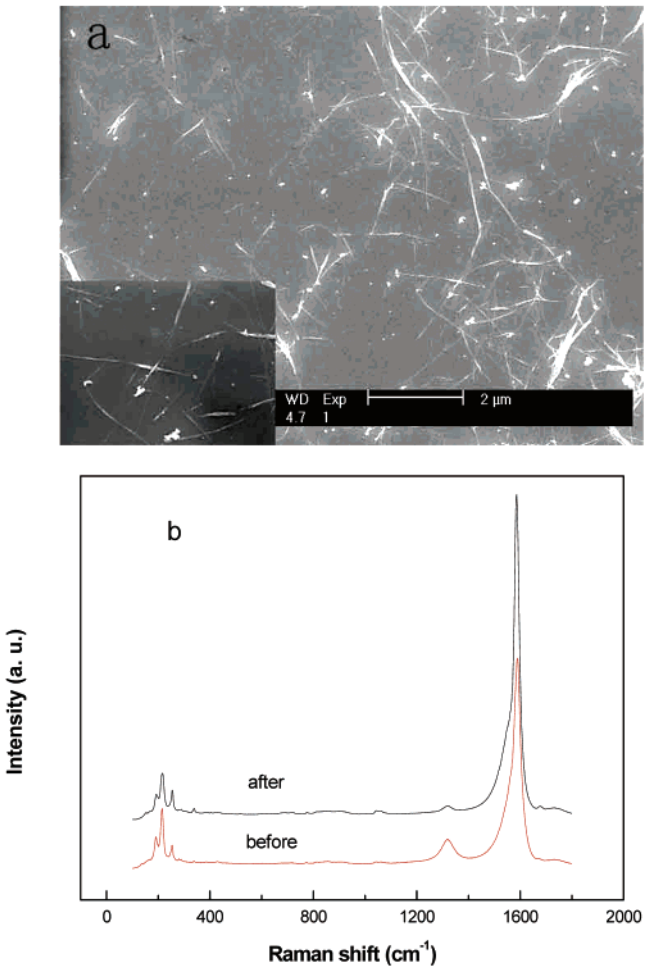

Figure 6. SEM image of the location of TiO_2 nanoparticles on gas-phase oxidation SWNTs (a; inset shows a magnified view) and the Raman spectra of SWNTs before and after gas-phase oxidation in air at 500 °C for 1 h (b).

that on refluxed SWNTs and gas phase oxidized SWNTs, indicating a greater number of defects present on the oxidized tubes. The tubes were also substantially shortened after the sonication process. Furthermore, statistical analysis revealed that interparticle separation on SWNTs prepared using the sonication method fell in the range between 50 and 500 nm, with an average distance of ~103 nm (Figure 7b), clearly demonstrating greater particle density. It is therefore possible that oxidation of SWNTs by sonication in H_2SO_4/H_2O_2 generates a greater number of carboxylic acid groups,[41]not only at defect sites already present in the tubes but also at newly created defect sites along the walls of SWNTs induced by the sonication process.[42] However, the SWNTs treated with H_2SO_4/H_2O_2 tend to form bundles during the sonication process (see inset of Figure 7a), resulting in the higher density of nanoparticles. This may be attributed to the hydrogen bonding between the carboxylic acid groups of the oxidized SWNTs. Given these results, refluxing in 2.6 M HNO_3 can be considered as a mild oxidation compared with sonication in H_2SO_4/H_2O_2. In other words, refluxing in 2.6 M HNO_3 merely oxidized defects already present in SWNTs and caused no severe damage to SWNTs.

FT-IR spectra provide further evidence for the differences between the oxidation processes used here. Figure 8 shows FTIR spectra of SWNTs treated with the different oxidiation processes. All the spectra show a peak at 1589 cm^{-1}, corresponding to the IR active phonon mode of SWNTs irrespective of the oxidation procedure used.[20] The intensity of the peak around

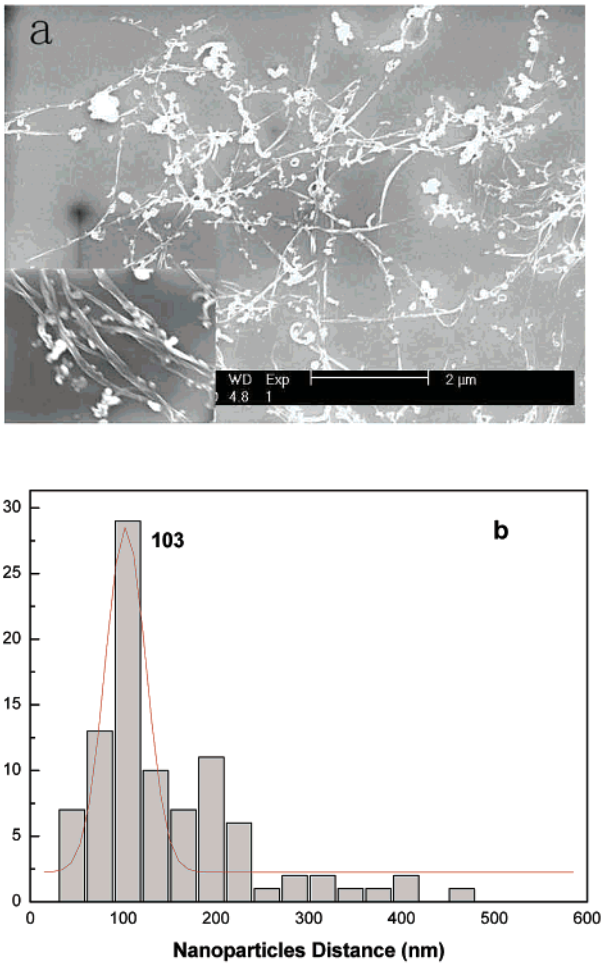

Figure 7. SEM image of the location of TiO_2 nanoparticles on SWNTs treated with sonication in H_2SO_4/H_2O_2 (a; inset shows a magnified view) and the corresponding histogram of the TiO_2 nanoparticle distances on SWNTs (b). The solid lines correspond to Gaussian fits.

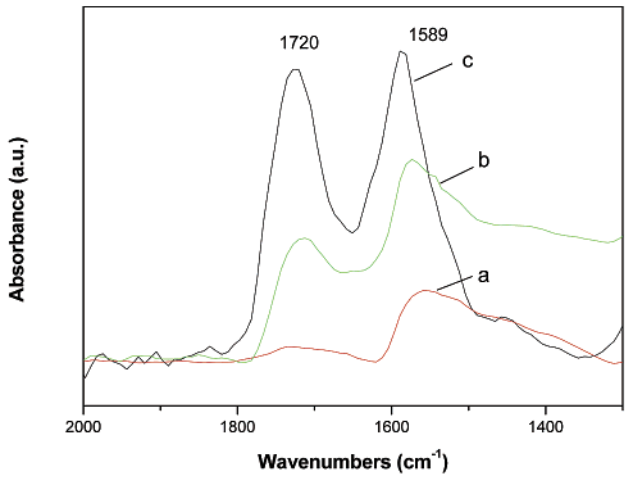

Figure 8. FTIR spectra of the SWNTs treated with different oxidation process: (a) gas-phase oxidation, (b) refluxing in 2.6 M HNO_3, and (c) sonication in H_2SO_4/H_2O_2.

1720 cm^{-1} is assigned to the stretch mode of carboxylic acid groups.[24] However, it was found to vary according to the oxidation process used. Sonication in H_2SO_4/H_2O_2 created the most carboxylic acid groups on SWNTs (Figure 8c). In contrast, gas phase oxidation produced hardly any carboxylic acid groups (Figure 8a). This result is in close agreement with the adsorption behavior of TiO_2 nanoparticles on the oxidized SWNTs. The greater the number of carboxylic acid groups contained on SWNTs, the greater the chemical adsorption of TiO_2 nanoparticles. However, IR measurements can only provide a macroscopic estimate of the defect density on SWNTs. By using the proposed nanoparticle method, the density, distribution, and ultrastructural location of the defects on SWNTs can be directly observed. Furthermore, TiO_2 semiconductor nanocrystals are known as quantum dots whose intrinsic properties are electronically configurable.[43] Once oxidized SWNTs have been reacted with them to form nanoscale heterojunctions, and such novel nanostructures will have the potential for tailoring the electronic properties of SWNTs and, subsequently, their application in nanoelectronic devices.

Conclusion

We have demonstrated that well-defined TiO_2 nanoparticles can be used to label defect sites on oxidized SWNTs via chemical adsorption between carboxylic acid groups of SWNTs and surface hydroxyl groups on the titanium dioxide nanoparticles via the formation of ester-like bonds. This method is potentially useful not only as a rapid tool to reveal the defect location on SWNTs but also to directly determine defect density. Moreover, the strategy is readily extended to generate a heterojunction incorporating nanotubes and nanoparticles. Further studies are currently underway to examine the effect of such heterojunctions on the electronic properties of SWNTs.

Acknowledgment. We are grateful for the financial supports from National Natural Science Foundation of China (NSFC 90206023, 59910161982, 29973001, 30000044), Ministry of Science and Technology of China (2001CB6105), and SRF for ROCS, SEM. We are also grateful to Prof. J. Kirkham (University of LEEDS) for her kind help and useful discussion.

References and Notes

(1) de Heer, W. A. de; Chatelain, A.; Ugarte, D. *Science* **1995**, *270*, 1179.
(2) Fan, S.; Chapline, M. G.; Franklin, N. R.; Tombler, T. W.; Cassel, A. M.; Dai, H. *Science* **1999**, *283*, 512.
(3) Bockrath, M.; Cobden D. H.; McEuen P. L.; Chopra, N. G.; Zettel, A.; Thess, A.; Smalley, R. E. *Science* **1997**, *275*, 1922.
(4) Tans, S. J.; Verschueren, A. R. M.; Dekker, C. *Nature* **1998**, *393*, 49.
(5) Schadler, L. S.; Giannaris, S. C.; Ajayan, P. M. *Appl. Phys. Lett.* **1998**, *73*, 3842.
(6) Wong, S. S.; Harper, J. D.; Lansbury, P. T., Jr.; et al. *J. Am. Chem. Soc.* **1998**, *120*, 603.
(7) Iijima, S.; Ichihashi, T. *Nature* **1993**, *363*, 603.
(8) Chico, L.; Lopez Sancho, M. P.; Munoz, M. C. *Phys. Rev. Lett.* **1998**, *81*, 1278.
(9) Kostyrko, T.; Bartkowiak, M.; Mahan, G. D. *Phys. Rev. B* **1999**, *59*, 3241.
(10) Rochefort, A.; Avouris, P. *J. Phys. Chem. A* **2000**, *104*, 9807.
(11) Sim, H. S.; Park, C. J.; Chang, K. J. *Phys. Rev. B* **2001**, *63*, 073402.
(12) Charlier, J. C.; Iijima, S. *Topics Appl. Phys.* **2001**, *80*, 55.
(13) Dai, H. *Topics Appl. Phys.* **2001**, *80*, 29.
(14) Monthioux, M.; Smith, B. W.; Burteaux, B.; Claye, A. *Carbon* **2001**, *39*, 1251.
(15) Koshio, A.; Yudasaka, M.; Iijima, S. *Chem. Phys. Lett.* **2001**, *341*, 461.
(16) Biro, L. P.; Gyulai, J.; Mark, G. I. *Micron* **1999**, *30*, 245.
(17) Kiang, C. H.; Goddard, W. A.; Beyers, R.; Bethune, D. S. *J. Phys. Chem.* **1996**, *100*, 3749.
(18) Liber, C. M. *Science* **2001**, *291*, 283.
(19) Mawhinney, D. B.; Naumenko, V.; Kuznetsova, A.; Yates, J. T., Jr.; Liu, J.; Smalley, R. E. *Chem. Phys. Lett.* **2000**, *324*, 213.
(20) Hamon, M. A.; Hu, H.; Bhowmik, P.; Niyogi, S.; Zhao, B.; Itkis, M. E.; Haddon, R. C. *Chem. Phys. Lett.* **2001**, *347*, 8.
(21) Fan, Y. W.; Burghard, M.; Kern, K. *Adv. Mater.* **2002**, *14*, 130.

(22) Hwang, K. C. *J. Chem. Soc. Chem. Commun.* **1995**, *2*, 173.
(23) Liu, J.; Rinzler, A. G.; Dai, H.; Hafner, J. H.; Bradley, R. K.; Boul, P. J.; Lu, A.; Iverson, T.; Shelimov, K.; Huffman, C. B.; Rodrigusz-Macias, F.; Shon, Y. S.; Lee, T. R.; Colbert, D. T.; Smalley, R. E. *Science* **1998**, *280*, 1253.
(24) Chen, J.; Hamon, M. A.; Hu, H.; Chen, Y.; Rao, A. M.; Eklund, P. C.; Haddon, R. C. *Science* **1998**, *282*, 95.
(25) Mawhinney, D. B.; Naumenko, V.; Kuznetsova, A.; Yates, J. T., Jr.; Liu, J.; Smalley, R. E. *J. Am. Chem. Soc.* **2000**, *122*, 2383.
(26) Hernadi, K.; Siska, A.; Thien-Nga, L. *Solid State Ionics* **2001**, *141*, 203.
(27) Kyotani, T.; Nakazaki, S.; Xu, W. H.; Tomita, A. *Carbon* **2001**, *39*, 782.
(28) Lawless, D.; Kapoor, S.; Meisel, D. *J. Phys. Chem.* **1995**, *99*, 10329.
(29) Falaras P. *Sol. Energ. Mater. Sol. Cells* **1998**, *53*, 163.
(30) O'Regan, B.; Grtzel, M. *Nature* **1991**, *353*, 737.
(31) Argazzi, R.; Bignozzi, C. A.; Heimer, T. D.; Castellano, F. N.; Meyer, G. J. *J. Phys. Chem. B* **1997**, *101*, 2591.
(32) Galoppini, E.; Guo, W.; Zhang, W.; Hoertz, P. G.; Qu, P.; Meyer, G. J. *J. Am. Chem. Soc.* **2002**, *124*, 7801.
(33) Bond, A. M.; Miao, W.; Raston, C. *Langmuir* **2000**, *16*, 6004.
(34) Ren, Y. J.; Zhang, Z.; Gao, E. Q.; Fang, S.; Cai, S. M. *J. Appl. Electrochem.* **2001**, *31*, 445.
(35) Li, Q. W.; Yan, H.; Cheng, Y.; Zhang, J.; Liu, Z. F. *J. Mater. Chem.* **2002**, *12*, 1179.
(36) Bahr, J. L.; Yang , J.; Kosynkin, D. V.; Bronikowski, M. J.; Smalley, R. E.; Tour, J. M. *J. Am. Chem. Soc.* **2001**, *123*, 6536.
(37) Liu, Z. F.; Shen, Z. Y.; Zhu, T.; Hou, S. F.; Ying, L. Z.; Shi, Z. J.; Gu, Z. N. *Langmuir* **2000**, *16*, 3569.
(38) Stahl, H.; Appenzeller, J.; Martel, R.; Avouris, P.; Lengeler, B. *Phys. Rev. Lett.* **2000**, *85*, 5186.
(39) Liang, W.; Bockrath, M.; Bozovic, D.; Hafner, J. H.; Tinkham, M.; Park, H. *Nature* **2001**, *411*, 665.
(40) Rao, A. M.; Richter, E.; Bandow, S.; Chase, B.; Eklund, P. C.; Williams, K. A.; Fang, S.; Subbaswamy, K. R.; Menon, M.; Thess, A.; Smalley, R. E.; Dresselhaus, G.; Dresselhaus, M. S. *Science* **1997**, *275*, 187.
(41) Sano, M.; Kamino, A.; Okamura, J.; Shinkai, S. *Science* **2001**, *293*, 1299.
(42) Koshio, A.; Yudasaka, M.; Zhang, M.; Iijima, S. *Nano Lett*. **2001**, *1*, 361.
(43) Brus, L. E. *Appl. Phys. A* **1991**, 53, 463.